Molecular Simulation of the Interface between Two Immiscible Electrolyte Solutions

Pedro Alexandrino Fernandes, M. Natália D. S. Cordeiro,* and José A. N. F. Gomes

CEQUP/Department Química, Faculdade de Ciências da Universidade do Porto, Rua do Campo Alegre 687, 4169/007 Porto, Portugal

Received: July 19, 2000; In Final Form: October 26, 2000

In this paper we analyze the properties of an interface between two immiscible electrolyte solutions. The study is conducted using high concentrations of an ionic salt in the aqueous phase (1 and 3 mol·dm^{-3} $MgCl_2$). The profile of the electric potential drop across the interface is calculated, and it is concluded that the surface potential is originated by the orientational anisotropy of the solvents near the interface. The ionic density profile shows a monotonic decrease as the ions approach the interface. The resultant ionic net charge density was found to be null across all the simulation box, within statistical uncertainty, confirming that the potential drop is only caused by the orientation of the solvent molecules. The orientational structure of the solvents is not disturbed by the presence of the ions. The radial distribution functions for the hydration shell of the ions show that the hydration shell remains almost unaffected at the interfacial region. The hydration number is reduced with the increase of the ionic concentration, a fact explained by the decrease of the H_2O/ion ratio. Ionic diffusion is anisotropic in all extension of the simulation box, being slower toward the interface than parallel to it. This anisotropy is due to the existence of an impenetrable barrier to displacements normal to the interfacial plane. It was also observed that the diffusion near the interface was faster than in the bulk solution. This effect is mainly caused by the smaller density of the interfacial region.

I. Introduction

The interface between two immiscible electrolyte solutions has been a subject of investigation for more than a century. The wide range of physical, chemical, and biological phenomena that are directly related to them justifies the research effort that is still presently being done to understand the peculiar properties of those systems. Liquid chromatography, mass transport across liquid phases, interfacial catalysis, drug delivery to the cells, or extraction processes are a few examples of important scientific problems which cannot be fully understood without a rigorous characterization of the interfacial region.[1−4]

Besides, there is an inherent fundamental interest in the study of biphasic systems, since they present a set of peculiar and exclusive properties. The original characteristics of the interfacial zone are generated by the discontinuous variation in many properties at the interfacial region, namely the composition, dielectric constant, as well as the anisotropic orientational structures of the solvents, and the specific associations between the immiscible solvents. Experimentally, the microscopic characterization of the interfacial region is a quite difficult task, since the interface corresponds to a zone of only several angstroms of thickness, which makes the limitation of the experimental probing to this sharp region a serious problem. Spectroscopic measurements, which are the experimental methods that provide more direct molecular information, are difficult to apply in those systems, since most of them do not distinguish the bulk molecules from the interfacial molecules. In that context, the received signal is originated mainly by the overwhelmingly most abundant molecules, the bulk ones. This problem can be overcome in the study of highly surface active substances, if they are almost only located at the interface, but not in the study of the solvents themselves, or in the study of most surface active agents, which are not exclusively located at the interface.

Therefore, until recently, only macroscopic properties such as the interfacial tension or electrochemical and transport properties have been successfully measured.

Recently, second-order spectroscopic methods (e.g.: sum frequency spectroscopy and second harmonic generation) have made possible the analysis of some interfacial properties, such as the orientational ordering of surfactants at the interface, the chemical composition of the materials adsorbed at the interface, adsorption/disadsorption kinetics, or the orientational ordering of the water molecules at the liquid|vapor interface.[5−9] In those methods the resultant signal comes only from the molecules located at noncentrosymmetric media, i.e., the molecules located at the interfacial region.

Another recent advance corresponds to the first direct measurement of the width of a liquid|liquid interface by Mitrinovic et al.[10] The measurement was performed using a X-ray reflectivity technique, and resulted in an average width of 3.3 Å, in clear agreement with previous theoretical calculations. However, it is not clear if the method distinguishes the intrinsic interfacial width, resulting from the discontinuity of the matter, from the extrinsic width caused by the more global interfacial capillary waves.

As the experimental probing of the microscopic interfacial properties is still very limited, a significant part of the present knowledge about interfacial structure and dynamics comes from theoretical methods, namely molecular dynamics and Monte Carlo computer simulations.

These methods have direct access to molecular-level information, are adequate to study a wide range of interfacial thermodynamic, dynamic, and structural properties, and are able to relate them to the distance from the interface. They have been applied to the study of the more commonly used interfacial

* Corresponding author.

10.1021/jp002571j CCC: $20.00
Published on Web 01/16/2001

systems, as the water|nitrobenzene, water|1,2-dichloroethane, water|chloroform, or water|2-heptanone systems.[11−14]

However, these theoretical studies have been restricted so far to the analysis of pure-solvent interfacial systems, neglecting the supporting electrolytes employed in experimental methods, but the supporting electrolytes are fundamental to performing one of the most important applications of two-phase chemistry, the transfer of ions between the two phases.

As most ions do not diffuse spontaneously from one phase to the other (the inorganic ions do not diffuse to the organic solvent and the organic ions do not diffuse to water), the application of an external electric field becomes necessary, using a pair of electrodes, each one in one of the phases. The supporting electrolyte is thus used to decrease the resistance of the solutions.

A proper interpretation of experimental results based in theoretical calculations must be done with simulations that reproduce in the most similar way the experimental environment. These observations motivated the present work, where the supporting electrolyte is included in the system. To begin with, the simulations were performed in the absence of external electric fields.

Magnesium chloride was the chosen supporting electrolyte, since it is commonly used in liquid|liquid electrochemical studies. The simulations are directed toward the study of concentrated electrolyte solutions, namely 1 and 3 mol·dm^{-3}. Usual experimental concentrations range from 0.005 mol·dm^{-3} up to about 2 mol·dm^{-3}. The study of the more diluted cases by computer simulations is still not possible presently, due to the enormous computational power needed to average the properties of less abundant species such as the ions at low concentrations.

In the organic phase, however, the concentration of the supporting electrolytes cannot be so high as in the water phase, since the solubility of the organic ions is very small, usually less than 0.005 mol·dm^{-3} in 2-heptanone. Even in the case of the more soluble organic salt in 2-heptanone that can be used in electrochemical processes, tetrahexylammonium 4-chlorotetraphenyl borate, the concentration employed experimentally does not exceed 0.01 mol·dm^{-3}. Under these conditions, our system is too small to include even one tetrahexylammonium 4-chlorotetraphenyl borate ionic pair (to include one ionic pair reproducing a concentration of 0.01 mol·dm^{-3} the simulated system should be 3 times larger, containing at least 702 HPT2 molecules, which is far beyond computational power). In addition, the importance of one ionic pair among 702 HPT2 molecules is negligible, especially considering that the ions do not approach the interface in the field-free case, and the large dimension of the ions, which hinders the approximations of the charged atoms to the water phase. Therefore, it seems more realistic not to include the organic ion in the HPT2 phase.

This paper is organized as follows. The water, HPT2, and ionic models, the potential functions, and the details of the simulations are outlined in the next section. Section III presents the results obtained in this study. Thermodynamic, structural, and dynamic properties of both solvents and of the supporting electrolyte are discussed, in bulk regions and at the interface. In section IV a picture of the properties of our interfacial system is drawn, based on the results reported in the previous section.

II. Computational Model

A. Molecular Models and Potentials. The water molecules were described by the well-known SPC model.[15]

The HPT2 molecules were modeled using the united atom formalism, where the CH_n ($n = 1, 2, 3$) groups are replaced by one interaction site centered on the C atom, with an interaction potential that reproduces implicitly the interactions of the individual atoms that constitute the united atom. This procedure generates a molecular model with eight interaction sites.

All bond lengths of the HPT2 molecule were held fixed, by applying the SHAKE algorithm[16] with a preset tolerance of 10^{-8} Å. As the water molecules were treated as rigid bodies, using the quaternion formalism, the suppression of the HPT2 vibrational degrees of freedom allowed us to integrate the equations of motion with a time step of 2 fs, resulting in a better sampling of the configurational space. It should be mentioned that previous studies showed that these bond constraints do not affect the properties studied in this kind of simulation.[17] All bond angles and dihedrals were considered flexible, and were parametrized using the CHARMm intramolecular force field parameters.[18]

The HPT2 intermolecular potentials are pairwise additive and include Coulombic and Lennard-Jones terms. The parameters for Lennard-Jones potentials were taken from the AMBER force field.[19] (To see a comparison of the quality of the CHARMm and AMBER intermolecular force fields, see ref 17.)

The parameters for the Coulombic potential of the HPT2 molecule (atomic charges) were derived from quantum calculations at the Hartree−Fock level, as previously reported.[17]

It should be also stressed that standard geometric combination rules were adopted to obtain the needed Lennard-Jones parameters for all interactions between different species.

The interaction potentials for the simulated ions (Mg^{2+} and Cl^-) also consisted in pairwise additive Lennard-Jones and Coulombic terms, whose parameters were taken from the literature.[20−22] The use of more accurate potentials, namely polarizable models for the ions, could be desirable. However, it would result in an increase in computational time that would make prohibitive this kind of calculations in systems with the dimensions considered here, even with modern computational resources (remember that a very large number of configurations must be sampled when the solutes are the species under study, since they are always the less abundant species of the system). However, the neglect of the explicit calculation of the polarization terms can be overcome by the use of effective potentials. In the case of the potentials employed here, it should be stressed that the parameters were refined to reproduce in aqueous solution the free energy of hydration, as well as the ion−water radial distribution functions. Therefore, those parameters include implicitly on average the ion−water polarization terms. The only missing term is the ion−ion polarization. However, this last term is not quantitatively very important, since the ion−ion interactions are much less important than the first and second hydration shell interactions. This can be indirectly confirmed by the results obtained in this work, where properties quite sensible to the quality of the interaction potentials, such as the density of the fluid, were found to be in close agreement with experimental results, confirming that our simple ionic models reproduce correctly the properties of the real systems.

B. Method. The water|HPT2 system was initially described by two rectangular boxes. One of the boxes contained a mixture of 234 HPT2 molecules with 21 water molecules, and the other one 1200 water molecules. In this way, the experimental concentration of water in saturated HPT2 was achieved. Both boxes had a cross section of 30 Å × 30 Å and a length that

reproduces the density of the corresponding pure liquids (respectively, 0.997 g/cm^3 for water and 0.8124 g/cm^3 for HPT2).

To enable volume variations, all production simulations were performed at 300 K and 1 bar in the NPT ensemble, using the Nosé-Hoover thermostat and barostat.[23,24] It should be noticed that, as the interfacial density is a priori unknown, if the initial volume was fixed it could induce serious spatial constraints that could influence the interfacial structure and the degree of mixing of the solvents near the interface.

An equilibration simulation of 200 ps was performed in both systems. Then, the two boxes were joined together along their cross sections (from now on, the *xy* plane in our internal frame) in one single box with the same cross section. The interactions between molecules belonging originally to different boxes were then slowly increased from zero to their final values during a 10 ps equilibration run, after which a new equilibration simulation was performed in the NVT ensemble during another 200 ps, using a Nosé-Hoover thermostat.

Then the ions were distributed homogeneously in the bulk aqueous phase. The ionic interaction potentials were slowly increased from zero to their final values in a 10 ps simulation. After the ionic potentials reached their definitive values, a new simulation of 200 ps was performed to allow for the equilibration of the hydration shells of the ions, as well as to achieve the equilibrium distribution of the ions in the aqueous phase.

After this, a new simulation of 150 ps was performed in the NPT ensemble, which was found to be enough to equilibrate again the system in this new ensemble. Then, the last configuration of the equilibrated system was used to start a simulation of 800 ps, from where the obtained results were taken.

The overall procedure was repeated, starting from different configurations of the two initial boxes, to obtain another 800 ps production simulation statistically independent of the first one. This procedure was used to analyze the ergodicity of the overall simulations (we can outline here that the results obtained in the two systems were equivalent within statistical accuracy). Therefore, the overall results were obtained from a total 1.6 ns simulation time.

All these procedures were repeated twice, considering two different electrolyte concentrations. In the fist set of simulations 22 $MgCl_2$ units were inserted in the bulk aqueous phase (22 Mg^{2+} cations and 44 Cl^- anions), and in the second set of simulations 66 $MgCl_2$ units were inserted in the bulk aqueous phase (66 Mg^{2+} cations and 132 Cl^- anions). This resulted in aqueous solutions with an average concentration of $MgCl_2$ of 1 and 3 mol·dm^{-3}.

A pair of simulations of 800 ps each was also performed in the NPT ensemble, starting from the configurations obtained previously, before the insertion of the ions, after a 150 ps equilibration period in the NPT ensemble. Those pure-solvent simulations will be used as a reference state to compare with the results obtained in the system containing the supporting electrolyte.

The integration of the equations of motion was performed using a Verlet leapfrog algorithm, with a time step of 2 fs. Periodic boundary conditions were applied in all three directions. The calculation of the long-range Coulombic forces was performed using the Ewald summation method with tinfoil boundary conditions. A molecular spherical cutoff of 14.5 Å was applied to the real part of the Ewald energy. For the short-range interactions a cutoff of 10 Å was employed.

A multiple time step algorithm[25] was used to evaluate interactions for distances larger than 10 Å, with a frequency of actualization of 10 fs. It was checked that this technique leads to good energy conservation (without thermostat) and did not affect the properties of the system.

When a box with two interfaces is used, care must be taken to prevent them from interacting. In those cases the simulation box must be long enough to ensure the independence between the interfaces. In our system the initial separation of the interfaces was 40 Å along the water phase and 61.68 Å along the HPT2 phase, i.e., 2.6 and 4.3 times greater than the long-range cutoff distance, which seems quite enough to avoid interfacial correlations.

All simulations were carried out using the dl_poly molecular dynamics package.[26]

III. Results

A. Density Profiles. In this section we present the results obtained for the density of the various species of the system as a function of the distance to the interface. The density profiles were calculated in slabs of 0.5 Å thickness parallel to the instantaneous geometry of the interface. The interfacial surface was derived by dividing the cross section of the simulation box into 25 square areas, with dimensions close to 6 Å × 6 Å (the exact length of the square side depends on the volume fluctuations), and calculating the position of the interface in each of the fractional interfacial areas. The position of the interface was considered to be the mean point between the interaction site of the HPT2 molecules closer to the water phase and the interaction site of the water molecules closer to the organic phase. In this last case the more advanced water molecules were only considered if the water concentration in that region was superior to the intrinsic solubility of water in HPT2 (1.41% (m/m)). Using the resultant 25 interfacial locations, the Gibbs dividing surface was generated, and the 0.5 Å thickness slabs considered were computed to be parallel, at each time step, to the interfacial surface. This procedure allows a better resolution in the calculation of properties that depend on the distance to the interface.[27] Figure 1 shows the results obtained for the pure solvents and for the electrolyte solutions, where the symmetry of the system was employed to improve statistics.

In the left graphic we can see three lines, corresponding to the density of the three simulated systems. No explicit distinction is made in the figure between the three lines because the results are almost graphically equivalent. There is only a visible difference between them that corresponds to a decrease in the water density in bulk water region in one of the simulations. Those results correspond to the 3 M $MgCl_2$ solution. The decrease in the water density is caused by the large number of ions in the bulk water phase that diminish the total number of water molecules present in that region. The same effect in the more dilute solution is less pronounced and not clearly demarked.

The solvent coexistence region, illustrated by the crossed decay of the density of both solvents near the interface, is influenced by the supporting electrolyte. It can be seen from the picture that the three lines are almost coincident. However, a detailed analysis of the picture shows that the coexistence region decreases as the electrolyte concentration increases. Thus, the outer line corresponds to the pure solvents simulation, the inner line corresponds to the simulation with the more concentrated electrolyte (3 M), and the middle lines correspond to the simulations with the 1 M supporting electrolyte. Magnesium chloride is a "structure making" electrolyte, acting as an aggregative agent in water, thus making the fluctuations in the position of the water phase near the interface smaller.

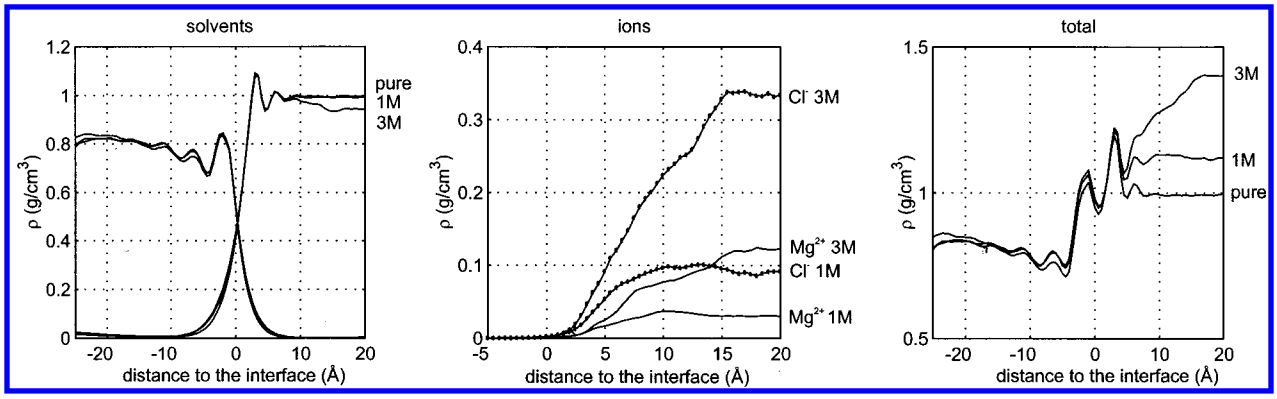

Figure 1. From left to right: density of the solvents, density of the ions, and total density. In the central picture the solid line corresponds to the cationic density and the dotted line corresponds to the anionic density. Negative distances to the interface correspond to distances measured from the organic phase. Positive distances correspond to distances measured from the aqueous phase.

Therefore, the thickness of the coexistence region decreases with the increase of the concentration of magnesium chloride. It must be stressed that, as demonstrated previously,[12−14,27] the coexistence region corresponds to a region that can be occupied by both solvents, but usually not simultaneously.

The center picture illustrates the ionic density profiles. It can be seen that ionic density decays steeply and monotonically near the interface. The diffusion of ions into the bulk HPT2 phase was never observed. The decay region is equivalent in extent for cations and anions at the same concentration (in fact, the number density of cations is half the number density of the anions throughout all the water phase). Bulk concentrations are achieved at about 15 Å from the interface for the 3 M solution and at about 10 Å from the interface to the 1 M solution.

The right graphic, relative to the total density of the system, exhibits clearly the oscillatory behavior of the density near the interface, demonstrating clearly the existence of a packing effect of each solvent against the opposite phase.

In the bulk region of the water phase, in the 1 M solution, the average density converges to a value of 1.123 ± 0.001 g·cm^{-3}, which is very close to the experimental value of 1.096 g·cm^{-3} [28] (relative deviation of 2.4%). In the bulk region of the water phase in the 3 M solution, the average density converges to a value of 1.357 ± 0.002 g·cm^{-3}, which is also close to the experimental value of 1.301 g·cm^{-3} [28] (relative deviation of 4.4%).

As the density is one of the properties more sensible to the quality of the intermolecular potential and to the accuracy of the simulations, we can conclude that the closeness between simulated and experimental results is a good evidence that the simulated systems reproduce correctly the behavior of the real systems, and the results should be considered realistic.

B. Surface Potential. The surface potential corresponds to a electrostatic potential difference between the two conducting liquid phases at equilibrium. In molecular simulations the surface potential can be directly computed using the mechanical definition.[29] In that sense, the interface potential can be attributed to the existence of nonzero charge density regions, caused either by a nonhomogeneous ionic distribution or by a nonisotropic orientation of the neutral solvent molecules. These nonzero charge density regions create an electric field that originates the potential drop. In this work the charge density was computed from the atomic partial charges, as a function of the distance to the interface, decomposed into solvent and solute contributions (due to the symmetry of the system the charge density computed parallel to the interface is null, within statistical uncertainty). The charge density along the *z* axis is then integrated to obtain the component of the electric field normal to the interface:

$$E_z(z) = \epsilon_0^{-1} \int_{\mathrm{HPT2}}^{\mathrm{H_2O}} \rho_q(z)\, \mathrm{d}z \qquad (1)$$

where $E_z(z)$ represents the *z* component of the electric field and $\rho_q(z)$ the charge density. The integration extends from the bulk organic phase to the bulk water phase. The potential drop across the interface ($\Delta\Phi(z)$) is then obtained by integration of the electrostatic potential

$$\Delta\Phi(z) = -\int_{\mathrm{HPT2}}^{\mathrm{H_2O}} E_z(z)\, \mathrm{d}z \qquad (2)$$

The interface potential was calculated for the three systems studied, and the obtained results are shown in Figure 2. It was concluded from the obtained charge density (and also from the results presented in Figure 2) that the contribution of the ions to the charge density is null, being the electric field generated by the anisotropic orientation of the solvent molecules near the interface. As mentioned in the next section, the water molecules at the interface point their hydrogen atoms toward the organic phase, making "hydrogen bonds" with the ketone oxygens, and placing their oxygen atoms directed toward the bulk aqueous phase. Thus, a test charge placed at the interface will be pushed to the interior of the water phase. As can be seen, the existence of the supporting electrolyte affects only very slightly the surface potential profile, causing the formation of a small minimum at the aqueous side of the interface, and diminishing the total potential drop. This minimum is produced by an inversion on the orientation of the water molecules in the inner region of the aqueous interface. This can be directly observed in the electric field profiles, where an inversion in the electric field occurs at nearly 2−3 water layers inside the water phase.

The HPT2 → H_2O potential drop is estimated as −1.1 V (pure solvents), −1.0 V (1 M $MgCl_2$) and −1.0 V (3 M $MgCl_2$).

The simple nature of the models indicates that the judgment about the quantitative value of the surface potential obtained in the simulations should be reserved.[30] The nonexistence of reliable experimental measurements of surface potentials does not help in making critical discussions about the quantitative aspects of the calculations (even for the simple case of the surface potential of the water liquid|vapor interface, the experimental measurements range from −1.1 to +0.5 V [30]). However, the qualitative aspects of the potential profile are physically reasonable and consistent with the observed orientational structure of the interfacial region, which in turn is much more well-defined and noncontroversial, both theoretically and

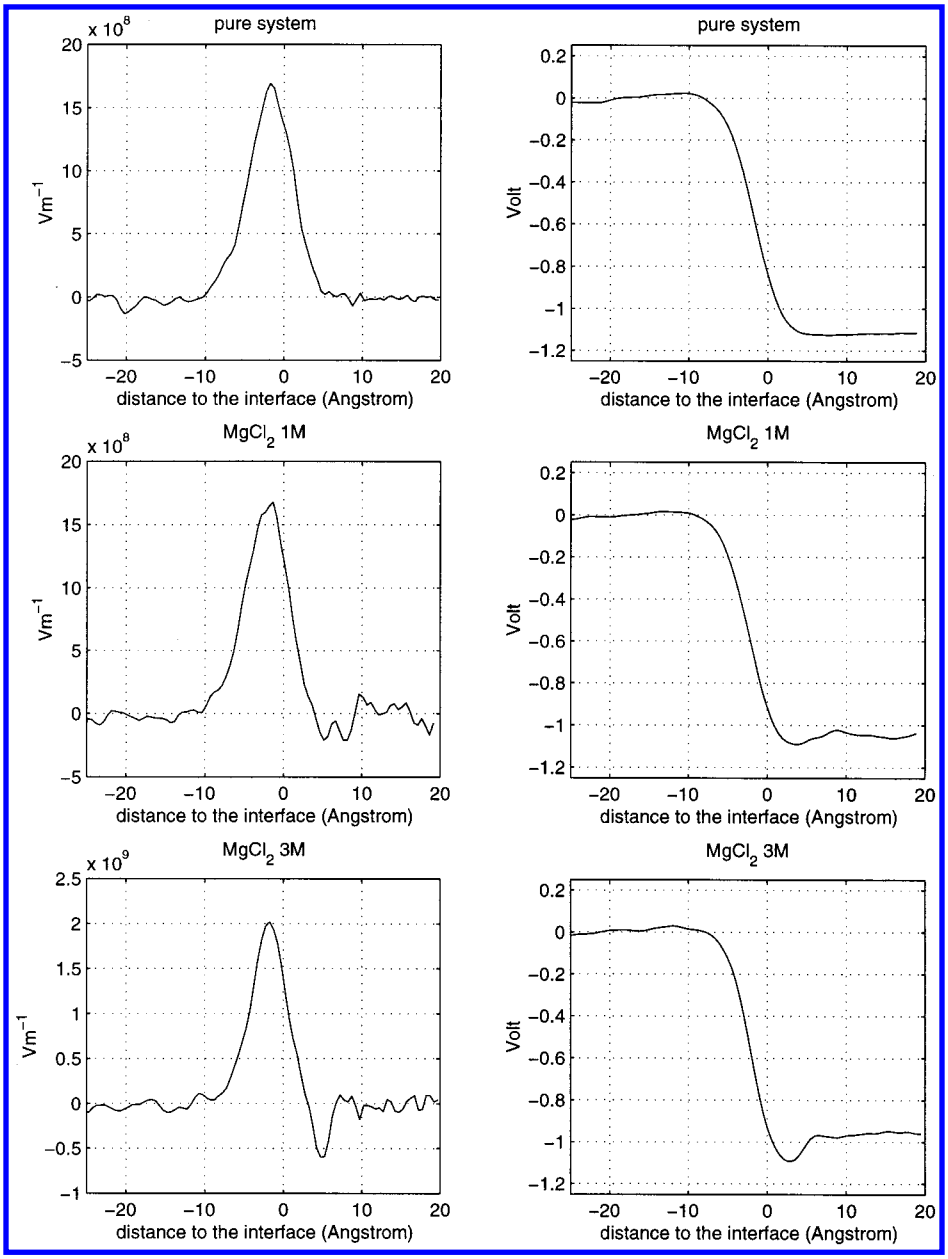

Figure 2. Left: Component of the electric field normal to the interface calculated in the pure solvents system (top), in the system with 1 M $MgCl_2$ (center), and in the system with 3 M $MgCl_2$ (bottom). Right: potential drop along the normal to the interface for the same systems.

experimentally. It must be stressed that the value of the surface potential is very sensible to the details of the electrostatic molecular model,[31,32] although the orientational molecular structure is not. The use of polarizable models should decrease the magnitude of the potential drop, as polarization works against the electric field.

The supporting electrolyte affects only slightly the generated electric field, confirming its origin in the anisotropic orientation of the solvent molecules.

C. Structure. In this section we begin by analyzing the specific orientation of the solvents near the interface. The results obtained in the electrolyte solutions are compared to the ones obtained in the pure system. The influence of the supporting electrolyte is discussed. Then, a study of the pair associations between both solvents, between the solvents and the solutes, and between the solutes is presented. Special attention is taken to the formation of ion pairs near the interface.

1. Orientational Structure. The orientational structure of the water molecules is determined by the calculation of the average *z* component of the molecular dipole moment along the normal to the interface. This quantity is calculated for the three systems considered and the obtained results are compared. To study the orientational structure of the HPT2 molecules, we calculated the average *z* component of the $\overrightarrow{O_K CH_3}$ vector, where O_K represents the ketone oxygen and CH_3 represents the opposite terminal methyl group of the molecule. Due to the symmetry of the system, the orientational distribution for the other components of the reference vectors (parallel to the interface) was found to be uniform, within statistical uncertainty. The obtained results are presented in Figure 3.

From Figure 3 we can see that the solvents are polarized at the interfacial region. The water molecules at the 2−3 water layers on the organic side of the interface point their dipoles toward the organic phase. The magnitude of the polarization increases as the water molecules penetrate into the organic phase and achieves a maximum value about 12%−13% above isotropic orientation. The magnitude of the polarization near the interface is not influenced by the presence of the ions, which

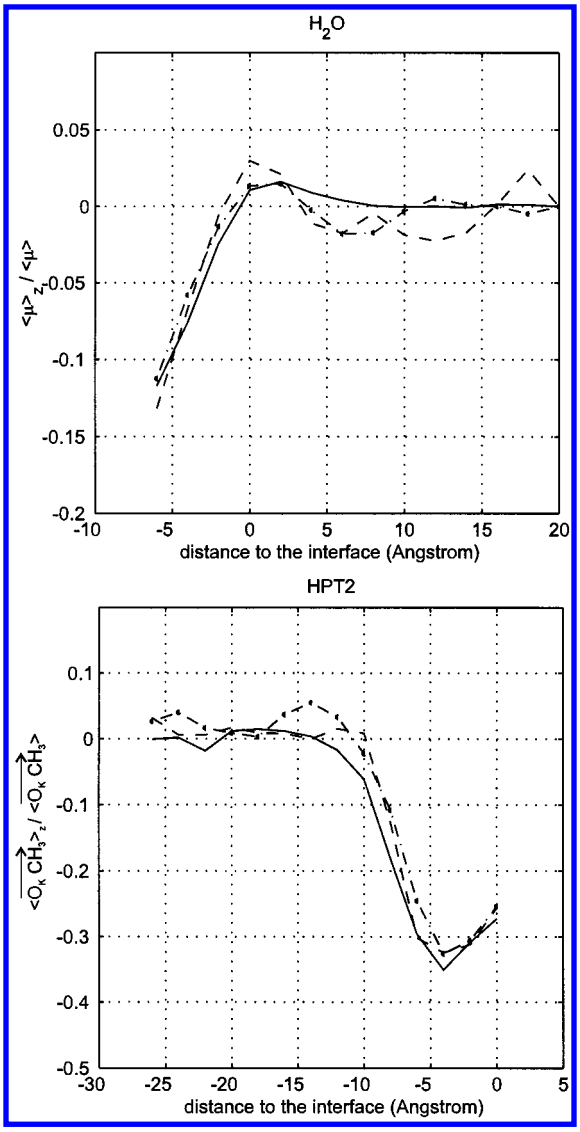

Figure 3. Top: normalized *z* component of the dipole moment of the water molecules, as a function of the distance to the interface. Bottom: normalized *z* component of the $\overrightarrow{O_K CH_3}$ vector as a function of the distance to the interface. The solid lines correspond to the results obtained in the pure system, the dotted lines correspond to the results obtained in the system containing 1 M $MgCl_2$, and the dashed lines correspond to the results obtained in the system containing 3 M $MgCl_2$.

are too far from the interface to directly influence the orientation of the interfacial water molecules. At the aqueous side of the interface and in bulk water phase the average *z* component of the water dipole moment approaches zero, which corresponds to either an isotropic orientation or an orientation parallel to the interfacial plane. In an earlier work the observation of the probability distribution for the *z* projection of the water dipole moment allowed us to distinguish which of the two hypotheses is correct, being concluded that the water orientation is isotropic in bulk water phase and is parallel to the interfacial plane in the aqueous side of the interface.[14] The larger fluctuations in the orientational distribution of the water molecules in bulk region when the supporting electrolyte is present can be attributed to the more constrained rotational movements that the aqueous solvent exhibits due to its coordination to the ions. In pure water, the rotational movements are more unrestricted and statistical orientational isotropy is more easily achieved.

The HPT2 molecules are also polarized at the interface, pointing their polar heads to the aqueous phase, to allow the establishment of hydrogen bonds with the water molecules. In this last case the anisotropy is more demarcated, and achieves a maximum value of about 30% above isotropic orientation. The degree of polarization is not influenced by the ions, by the same reasons as exposed above, and the results obtained in the three systems can be considered as equivalent.

Therefore, we can conclude that the orientational distribution of the solvents is not affected by the supporting electrolyte, even at concentrations up to 3 mol·dm^{-3}. The main reason for this observation relies on the fact that the ions do not approach very closely the interface to have a visible influence in the orientation of the solvents.

2. Pair Associations. In this section we explore the preferential pair associations established between the species in solution. Several radial distribution functions were calculated, and we decided to discuss only a reduced number of representative examples, namely the ones referring to the ion−oxygen and the cation−anion associations.

The simulation box was divided into slabs parallel to the interfacial plane with a thickness of 2.5 Å. Then, for each type of association, a radial distribution function was calculated independently for each slab. A radial distribution function is associated with a specific slab when its central atom is located inside the considered slab.

After obtaining a radial distribution function for each slab, a three-dimensional surface was generated, representing a radial distribution function dependent on the species separation and on the distance to the interface. The surface was generated using a triangle-based linear interpolation technique.

All the ion−water radial distribution functions were normalized by the bulk water density and all the $Mg^{2+}-Cl^-$ radial distribution functions were normalized by the bulk chloride density. The results are presented in Figures 4−6.

The radial distribution functions obtained in the 1 and 3 M systems are qualitatively similar, the major differences being in the quantitative aspects. Therefore, we decided to show the results obtained in only one of the two systems. The quantitative differences can be observed and discussed from the results presented in Figure 7, where the number of neighbors inside the first hydration shell is presented as a function of the distance to the interface. The coordination numbers were obtained by integration of the first peak of the corresponding radial distribution functions.

The analyzes of the results allow us to conclude the following:

a. Mg^{2+} Hydration. In the 1 M system the hydration shell of the Mg^{2+} ion is composed of an average number of 5.5 ± 0.1 water molecules, in good agreement with the experimental coordination number of 6 water molecules obtained using X-ray diffraction methods.[33−37] The coordination number is statistically constant throughout the bulk water phase. The first solvation shell is very robust and the hydration number decreases only after passing the interface. The location of the first peak in the radial distribution function corresponds to 2.0 Å, also in good agreement with experimental X-ray diffraction measurements that attribute to the $Mg^{2+}-O_w$ most probable distance values ranging from 2.00 to 2.12 Å.[33−37] The near presence of the organic phase does not affect the hydration geometry, as the location of the peak remains unchanged.

In the 3 M system the first hydration shell of the Mg^{2+} ion includes a more reduced number of water molecules, which grows from 4.1 in bulk water phase to 5.3 near the interface (on the organic side of the interface, the hydration number decreases to about 2.8). The smaller hydration number of Mg^{2+} in the more concentrated solution is due to the decrease in the number of water molecules *per* ion. This factor is not relevant

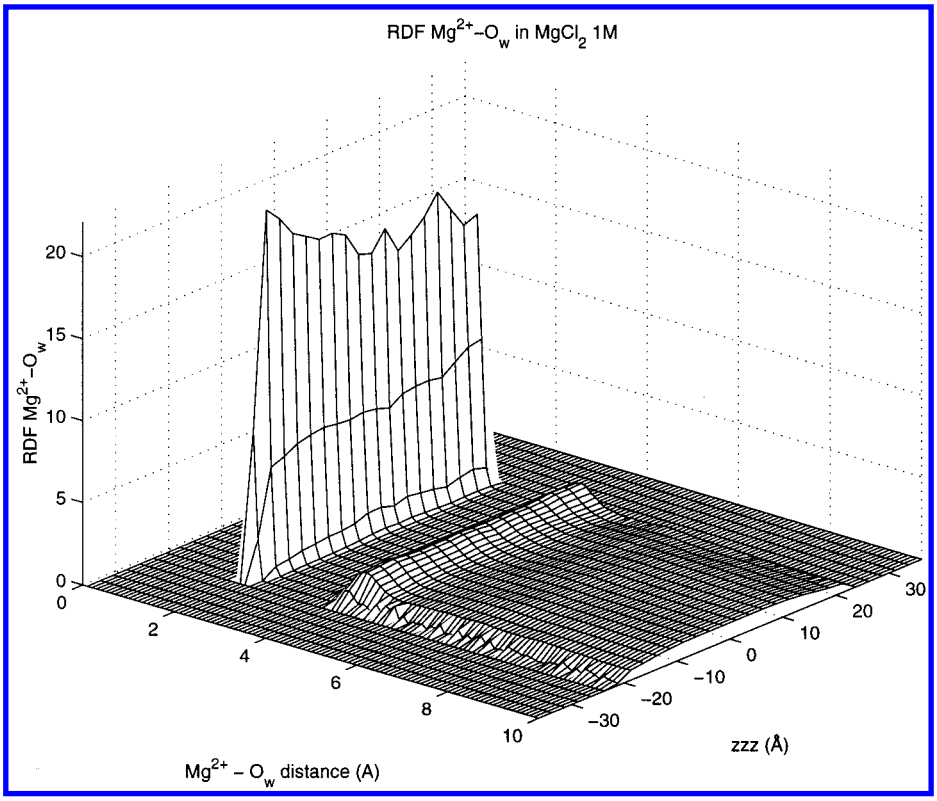

Figure 4. Mg^{2+}−oxygen radial distribution function in the 1 M system. The water phase occupies the region between $zzz = -20$ Å and $zzz = +20$ Å. In this picture the location of the molecules is given by their position in the z axis of the reference frame and not by their distance from the interface, as in the preceding pictures.

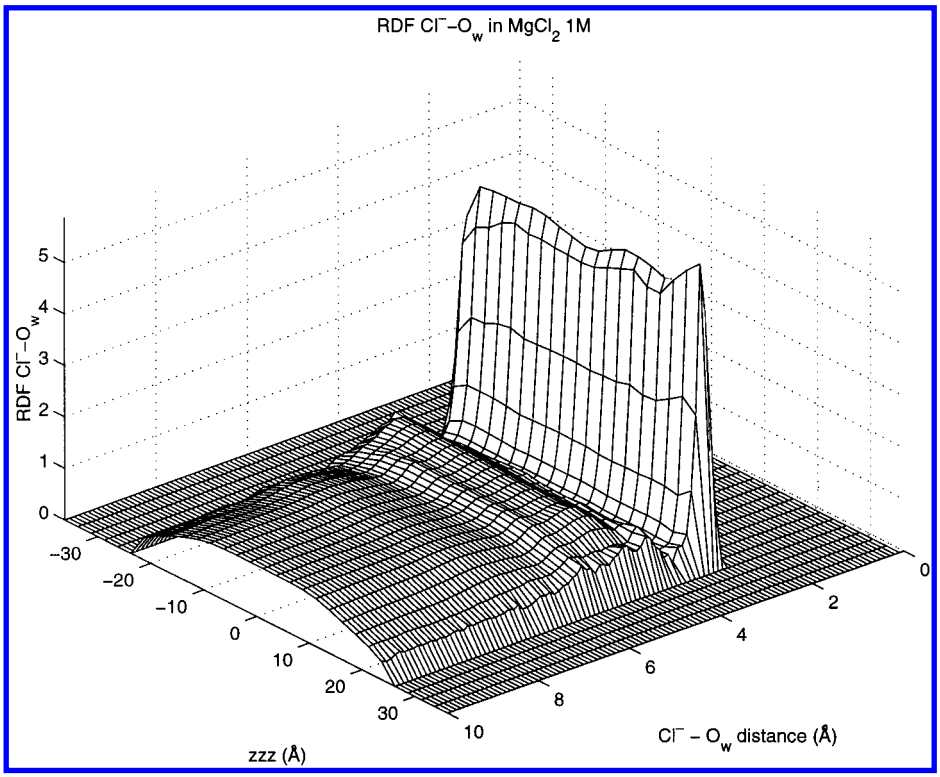

Figure 5. Cl^-−oxygen radial distribution function in the 1 M system. The water phase occupies the region between $zzz = -20$ Å and $zzz = +20$ Å. In this picture the location of the molecules is given by their position in the z axis of the reference frame and not by their distance from the interface.

in dilute solutions, where there is a large excess of water molecules, and the ions do not compete to coordinate water molecules, but becomes crucial in more concentrated solutions. In the present cases the H_2O/Mg^{2+} average ratio for the entire aqueous phase decreases from 54.5 in the 1 M solution to 18.2 in the 3 M solution. If we also consider the Cl^- ions, the ratio $H_2O/(Mg^{2+} + Cl^-)$ decreases from 18.2 in the 1 M solution to 6.1 in the 3 M solution.

The decrease of the average coordination number with the increase of the concentration, although chemically quite reason-

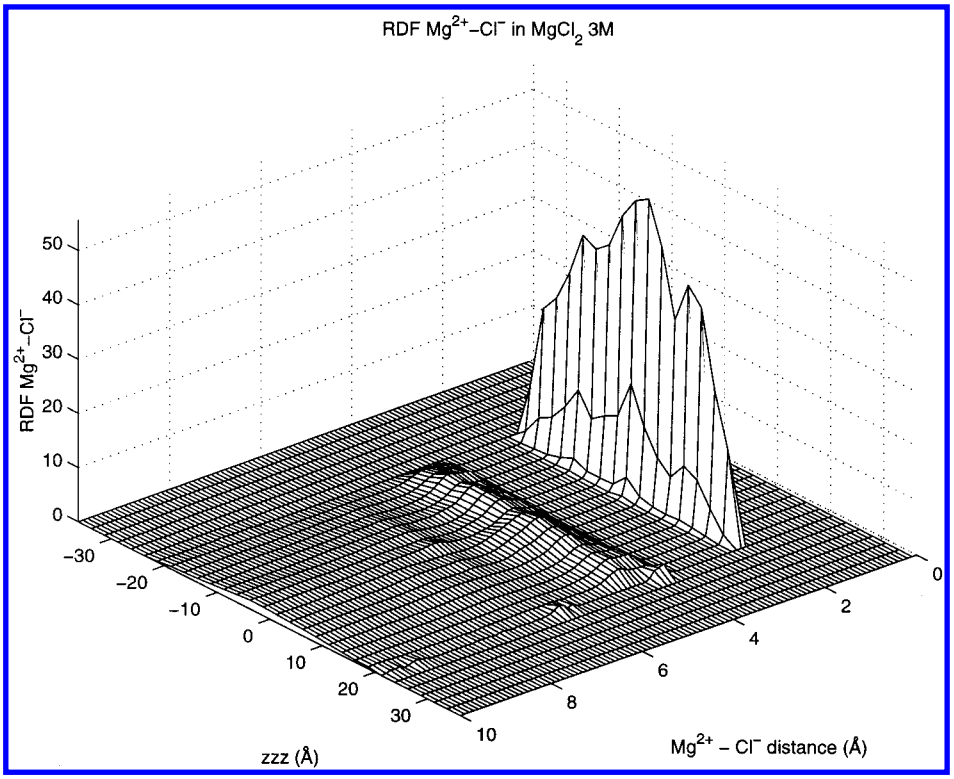

Figure 6. $Mg^{2+}-Cl^-$ radial distribution function in the 3 M system. The water phase occupies the region between $zzz = -20$ Å and $zzz = +20$ Å. In this picture the location of the molecules is given by their position in the *z* axis of the reference frame and not by their distance from the interface.

able and intuitively predictable, seems not to be in agreement with experimental findings, at least for the electrolyte considered. Indeed, it is surprising to note that this effect is not found in X-ray measurements, where the experimental hydration numbers obtained correspond to 6 in a electrolyte concentration range up to 4.8 M.[33−37] In the more concentrated $MgCl_2$ solution used on this kind of measurements[36] the ratio $H_2O/(Mg^{2+} + Cl^-)$ corresponds to 3.8 water molecules *per* ion. Thus, the only way to justify such a experimental result is to consider that the same water molecules belong simultaneously to the hydration shells of more than one ion. We believe that this last point deserves further investigation in the future.

The location of the first peak in the radial distribution functions is still in good agreement with experimental data, maintaining the same value found in the 1 M solution, whatever the location of the ion.

The increase in the hydration number of the Mg^{2+} ions in the more concentrated solutions near the interface is caused by the increase in the $H_2O/(Mg^{2+} + Cl^-)$ ratio in that region. Indeed, if we approach the interface from the bulk water phase, the ionic density decay starts as the ions approach the interface by less than ca. 15 Å, where the water density still corresponds to the bulk value. This leads to a marked increase in the number of water molecules accessible for each magnesium ion.

b. Cl^- Hydration. In the 1 M system the hydration shell of the Cl^- ion is composed of an average number of 7.1 ± 0.1 water molecules, in agreement with experimental coordination numbers obtained by X-ray diffraction that range from 5.9 to 8−8.2 water molecules.[35,37,38] The coordination number is statistically constant throughout the water phase. Similarly to the magnesium ion, the first solvation shell is very robust, not being affected by the closeness of the organic phase. The location of the first peak in the radial distribution function corresponds to 3.0 Å, in reasonable agreement with X-ray diffraction results that range from 3.1 to 3.15 Å.[39,35,37] Again, no change in the location of the peaks occurs near the interface.

In the 3 M system, the hydration number of the first coordination shell contains a smaller number of water molecules that grows from 6.5 in the bulk water region to 6.9 near the interface. As observed before for the Mg^{2+} ion, the hydration number increases near the interface due to the large increase in the H_2O/ion ratio. The decrease of the hydration number with the increase in the concentration is also observed, although to a smaller extent than for the case of the magnesium ion. The location of the first peak in the radial distribution function is found to be the same as in the less concentrated solution, and is independent of the location of the ion relative to the interface.

c. Ionic Associations. Associations between monatomic cations and anions are well-known experimentally.[40] The association consists of the replacement of one or more water molecules belonging to the hydration shell of a given ion by an opposite-charged ion. Those associations are favored at high electrolyte concentrations. Figure 6 illustrates the radial distribution function for the $Mg^{2+}-Cl^-$ associations. A very demarcated first peak reveals the existence of ionic associations in the correspondent solution. The same phenomenon is observed in the system containing the lower concentration (1 M) of $MgCl_2$.

Integration of the first peak of the obtained radial distribution functions allow us to calculate the average cation−anion coordination numbers. In the bulk solution with the lower concentration an average of 0.67 ± 0.07 chloride ions is associated to each magnesium ion. The most probable $Mg^{2+}-Cl^-$ distance, given by the location of the first peak, corresponds to 2.1 Å, very close to the location of the first peak in the $Mg^{2+}-$oxygen radial distribution function. The location of the peak is not affected by the approach to the interface, confirming that the ionic solvation geometry resists the approach to the organic phase.

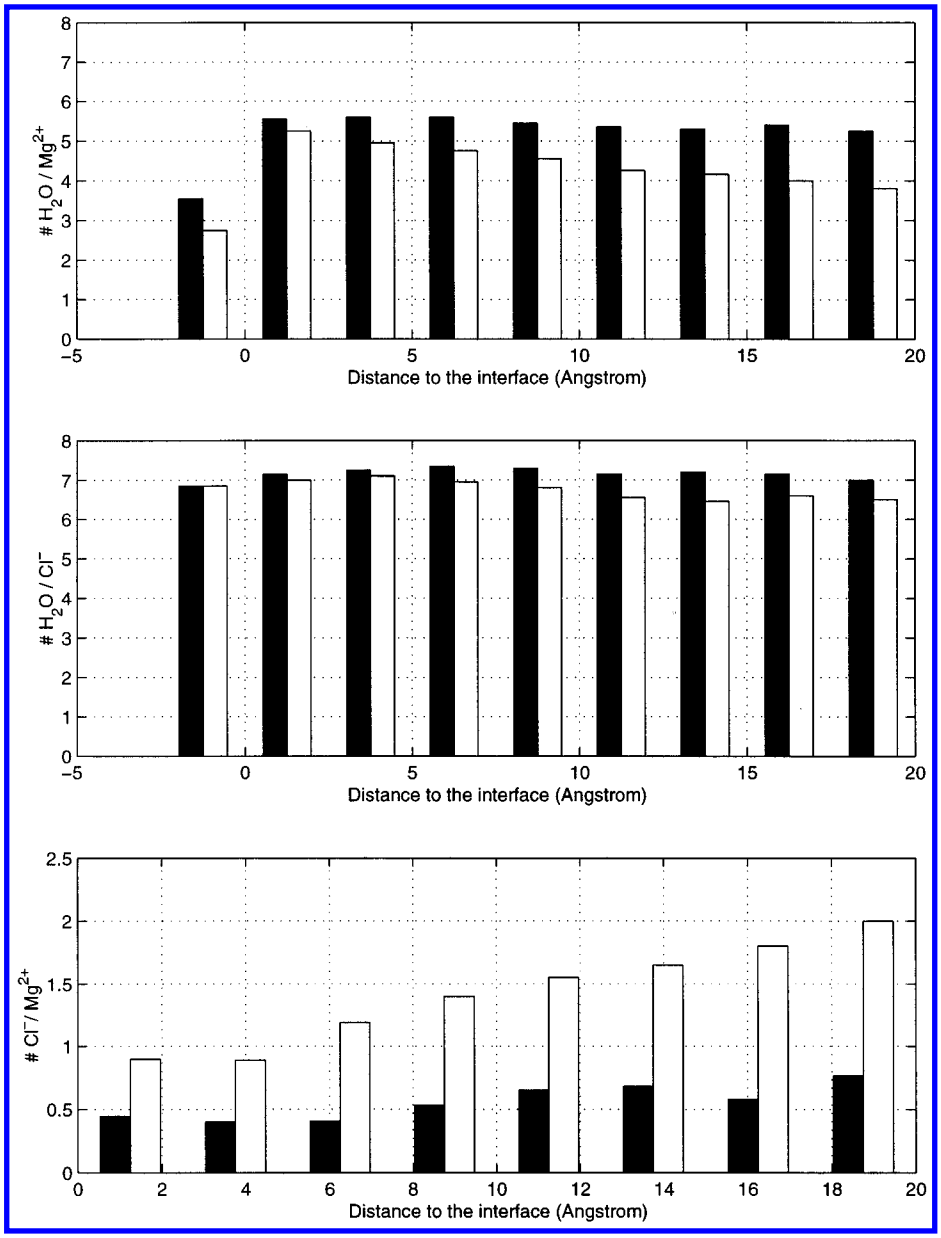

Figure 7. Coordination numbers for the hydration shells of the ions and also for the cation−anion associations. Black bars correspond to the results obtained for the 1 M system and white bars to the ones for the 3 M system.

The coordination number decreases as the ions approach the interface, a consequence of the decrease in the ionic density near the interface. Considering the water region closer than 4 Å from the interface, we find an average coordination number of 0.45 ± 0.04. This value is smaller than the value found in the bulk water region, due to the much smaller ionic density, but it is very high compared to the decrease in the ionic density in that region (13.5 times). Therefore, we can conclude that the Mg^{2+}−Cl^- associations are very robust, as they only decrease by a factor of 1.5 while the ionic density is reduced by a factor of 13.5.

In the 3 M system the average coordination number in bulk water region corresponds to 1.8 ± 0.1. The increase in the cation−anion coordination number compared with the preceding case is caused by the higher concentration of electrolyte. The coordination number decreases to an average of 0.9 ± 0.1 near the interface. The conclusions obtained considering the more dilute solution can also be applied here to explain the decrease in the ionic coordination number near the interface. Again, the decrease in the coordination number near the interface (2 times) is not proportional to the decrease in the ionic density in that region (17.2 times).

As far as we know, there are no experimental measurements of the ionic coordination number of magnesium chloride. However, we can compare our simulation results with results obtained in other similar systems, to check if the results are reasonable.

The ionic coordination number of Mg^{2+} in a solution of magnesium dihyrogenophosphate ($Mg(H_2PO_4)_2$) was measured using X-ray diffraction techniques. The results revealed the coordination of an average of 1.0 dihyrogenophosphate ions in a solution with an H_2O/Mg^{2+} ratio of 34.[41] A similar measurement was performed in solutions of magnesium acetate, with H_2O/Mg^{2+} ratios of 33.1 and 14.9, and a value of 0.8 acetate ions coordinated to each Mg^{2+} ion was found for both solutions.[42] The ionic coordination number of solutions of calcium chloride with H_2O/Ca^{2+} ratios ranging from 6.2 to 4.0 was measured using X-ray diffraction techniques. The coordination numbers increase with increasing concentration, from 0.9 to 2.1 coordinated chloride ions.[43]

Direct comparison of the experimental results with our theoretical estimations would not be correct, since measurements were made in different systems. However, it should be noted that experimental findings do not contradict theoretical results. More, qualitative agreement between experimental and theoretical results, at least for the magnitude of the phenomenon, seems to exist. Therefore, we conclude that the theoretical findings are reasonable and acceptable, and should be considered valid, although definitive quantitative conclusions should only be taken based on a comparison with experimental measurements performed in the same system.

D. Dynamics. In this section we aim to answer the following question: to what extent does the presence of the interface affect the dynamic properties of the supporting electrolyte? This seems to be a fundamental aspect for the comprehension of many important phenomena in biphasic chemistry. The kinetics of simple and assisted ion transfer processes, as well as the kinetics of general extraction processes, depends closely on the peculiar diffusive properties of the solutes near the interface. To get an answer to this question, we have calculated the diffusion coefficients for the ions as a function of their distance from the interface. Rotational kinetics, usually analyzed by calculation of the orientational correlation functions, was not studied here since the ions are monatomic, and treated as point masses. In addition, we have also calculated the mean residence time of the water molecules in the hydration shell of the ions near the interface and in bulk solution, to measure the influence of the interface under the stability of the hydration shell.

1. Diffusion Coefficients. The diffusion coefficients of the Mg^{2+} and Cl^- ions were calculated using the Einstein relation

$$D_\alpha = \lim_{t\to\infty} \frac{\Delta R_\alpha^2}{2t} \qquad (3)$$

where ΔR_α is the mean displacement in the α direction ($\alpha = x, y, z$), D_α corresponds to the α component of the diffusion coefficient, and t is the time. The results are presented in terms of the diffusion coefficients parallel (||) and normal ($\perp$) to the interfacial plane. The diffusion coefficients parallel to the interfacial plane correspond to the average between D_x and D_y, and the diffusion coefficients normal to the interface correspond to the D_z component of the diffusion coefficient. The calculations were performed separately for the bulk and interfacial regions. The bulk region corresponds to a slab of 10 Å thickness, parallel to the interfacial plane (the *xy* plane), located in the center of the box. The interfacial region corresponds to a slab of 10 Å thickness, parallel to the interfacial plane and centered at the interface (5 Å inside the water phase and 5 Å inside the organic phase). The calculations were performed for both systems studied, and the obtained results are presented in Table 1.

Besides the diffusion coefficients, the table also shows the ratio between diffusion parallel and normal to the interface and the ratio between diffusion in bulk and interfacial regions. From the results presented in the table several conclusions can be drawn:

(i) Ionic diffusion is anisotropic, being faster parallel to the interfacial plane than toward the interface. This conclusion holds for both ions and for both systems studied. The anisotropy is more pronounced in the system with the more concentrated electrolyte, and also more demarcated for the magnesium ion than for the chloride ion.

This phenomenon is caused by the existence of an incompressible and impenetrable barrier (the organic phase) that hinders the ionic displacements toward the interface. This effect is limited not to the interfacial region, but to all the extension of the simulation box. Indeed, in dense fluids it is easy to understand that this effect propagates into the bulk. Bulk ions have severe constraints in moving toward the interface because the molecules between them and the interface are also submitted to the same kind of constraints to approach the interface, which makes it quite difficult to open free spaces to the progression of the ions. This is the most long-range interfacial effect known, and a similar situation was also observed in analyzing the dynamics of the solvents.[14] To analyze the extent of this effect, it would be necessary to use much longer simulation boxes, which is not feasible even with modern computational resources.

TABLE 1: Diffusion Coefficients of the Mg^{2+} and Cl^- Ions Calculated Separately for the Parallel (||) and Normal ($\perp$) Components to the Interfacial Plane

$10^9 D$	Mg^{2+} bulk	Mg^{2+} int.	Cl^- bulk	Cl^- int.
1 M ||	0.88 ± 0.05	0.97 ± 0.03	1.24 ± 0.05	1.34 ± 0.02
1 M $\perp$	0.55 ± 0.02	0.61 ± 0.04	0.92 ± 0.04	1.07 ± 0.04
1 M ||/$\perp$	1.6	1.6	1.3	1.3
3 M ||	0.27 ± 0.02	0.49 ± 0.01	0.35 ± 0.01	0.76 ± 0.01
3 M $\perp$	0.13 ± 0.02	0.25 ± 0.01	0.21 ± 0.02	0.556 ± 0.007
3 M ||/$\perp$	2.1	2.0	1.7	1.4

bulk/int.	Mg^{2+} ||	Mg^{2+} $\perp$	Cl^- ||	Cl^- $\perp$
1 M	0.91	0.90	0.93	0.86
3 M	0.55	0.52	0.46	0.38

[a] The calculations were performed for the bulk water region and for in the interfacial region. All values in $m^2\ s^{-1}$.

(ii) Ionic diffusion is faster near the interface than in the bulk region, for either displacements parallel or perpendicular to the interfacial plane.

Diffusion in dense fluids is quite sensible to the density of the system, because the molecular displacements are limited by the near presence of other molecules. It was demonstrated in an earlier work[17] that an increase of 4.6% in the density of HPT2 can produce a decrease of 50% in the HPT2 self-diffusion coefficients. Therefore, the increase in the translational kinetics near the interface is mainly caused by the decrease in the density of the system in that region.

(iii) Diffusion is faster in the solution with the less concentrated electrolyte.

This effect was predictable and can be justified by the same reasons as the ones presented above. Hence, in the more concentrated solution, the density is far superior to the density in the less concentrated solution, which makes the translational kinetics slower.

Comparison between theoretical results and experimental data should be made considering the component of the diffusion coefficients parallel to the interfacial plane in the less concentrated solution. Those are the ones which are calculated in an environment more similar to experimental measurements. Indeed, experiments are performed in an isotropic media, and at very low electrolyte concentrations, to obtain the diffusion coefficients at infinite dilution. It would be interesting to have experimental data about those quantities as a function of the concentration of magnesium chloride, but as far as we know, there are no such data in the literature. Experimental diffusion coefficients for magnesium ion range between 0.7×10^{-9} and $1.1 \times 10^{-9}\ m^2\ s^{-1}$.[44,45] Therefore, the result obtained here ($(0.88 \pm 0.05) \times 10^{-9}\ m^2\ s^{-1}$) is in fair agreement with experimental data.

For the chloride ion we have obtained a value of $(1.24 \pm 0.05) \times 10^{-9}\ m^2\ s^{-1}$, which should be compared to the experimental value of $2.0 \times 10^{-9}\ m^2\ s^{-1}$.[46] Although not so

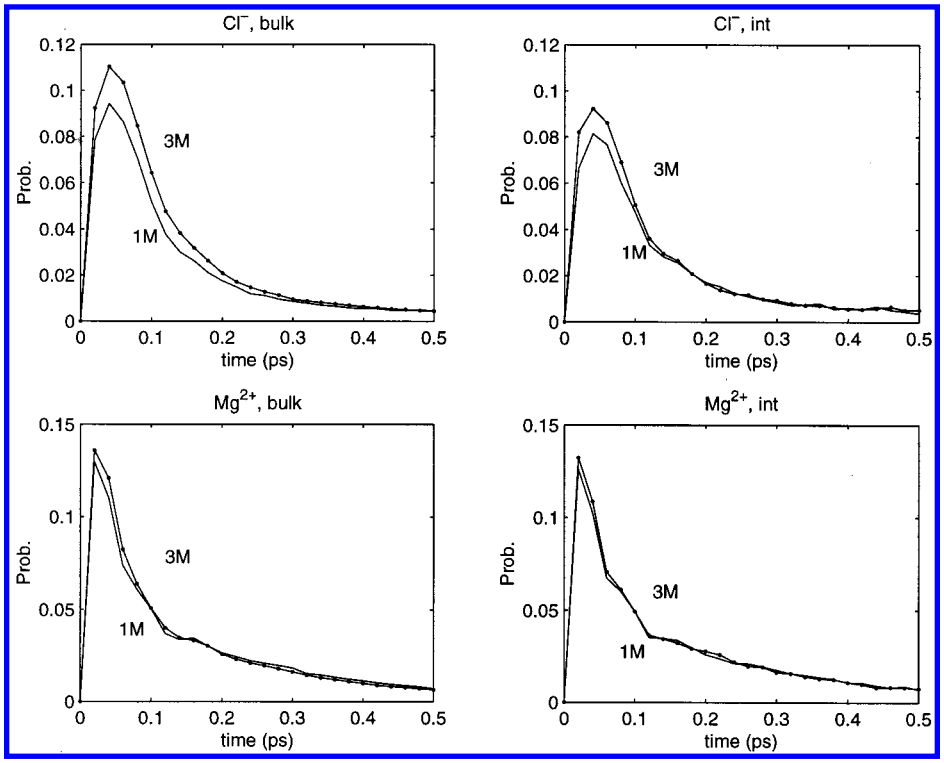

Figure 8. Details of the probability distribution for the residence time of the water molecules in the first hydration shell of Cl^- and in the second hydration shell of Mg^{2+}. The left graphics correspond to the residence time distributions in the bulk aqueous phase and the right graphics to the residence time distributions near the interface. The top graphics refer to the Cl^- ion and the bottom ones to the Mg^{2+} ion. In each picture the solid line corresponds to the results obtained in the 1 M solution and the dotted line to the 3 M solution.

precise as in the case of the magnesium ion, the result is in satisfactory agreement with experimental data. We must remember that the diffusion coefficients are one of the properties more sensible to the specific models employed. Even for the most optimized molecular models (the models used to simulate liquid water), the diffusion coefficients obtained in simulation deviate from experimental results typically by more than 50%.[46−48] Another factor that makes difficult the correct reproduction of the experimental diffusion coefficients is their straight dependence on the density of the system. Hence, a small deviation in the density of the fluid can produce a very large deviation in the diffusion coefficients, as discussed previously. However, those small quantitative details are not fundamental to the discussion here, where we are more concerned in obtaining a comparative description of the behavior of the diffusive kinetics of the ions near the aqueous interface, which can be fully achieved with the present models.

2. Mean Residence Time of Water in the Hydration Shell of the Ions. In this section we aim to investigate the mean residence time (MRT) of the water molecules in the hydration shell of the considered ions. This quantity was calculated for the first hydration shell of the chloride ion and for the second hydration shell of the magnesium ion. We have used the "direct route" to the calculation, which is described below.

We considered the residence time of a water molecule in the hydration shell of a given ion as the time elapsed since the water−ion distance becomes inferior to the radius of the corresponding hydration shell (given by the position of the minimum in the corresponding radial distribution function) until the moment in which the water−ion distance exceeds the hydration shell radius.

In this kind of calculations some authors consider the existence of a "transient time" in which the molecule can leave and return to the hydration shell without really achieving bulk properties.[49,50] In that case the water molecules still belong to the hydration shell of the ion if they leave and return to the hydration shell during a time period smaller than the transient time. Typical values for the transient time lie in the range of 0−2 ps. In our calculations we do not consider the concept of transient time, which corresponds to the use of a transient time of 0 ps.

TABLE 2: Mean Residence Times for the Water Molecules in the First Hydration Shell of Cl^- and in the Second Hydration Shell of Mg^{2+} (ps)

	Mg^{2+} bulk	Mg^{2+} int.	Cl^- bulk	Cl^- int
1 mol·dm^{-3}	0.889 ± 0.004	0.87 ± 0.03	1.69 ± 0.01	1.62 ± 0.04
3 mol·dm^{-3}	0.83 ± 0.02	0.81 ± 0.03	1.37 ± 0.03	1.55 ± 0.05

Using this definition, we calculated a probability distribution for the residence time of the water molecules in the hydration shell of the ions, and from that the average residence time was obtained. In Figure 8 we illustrate the probability distributions for the residence time of the water molecules in the first hydration shell of the chloride ion and in the second hydration shell of the magnesium ion. The picture illustrates details of the calculated probability distributions, for residence times smaller than 0.5 ps. The calculations were extended up to 800 ps. To define the bulk water region and the interfacial region, we used the same criteria as in the study of the diffusion coefficients (please, see section above).

The average residence times obtained are shown in Table 2. It was not possible to estimate the MRT of the water molecules in the first hydration shell of the magnesium ion, since it was far superior to the simulated time (800 ps). It was never observed during any of the simulations that even one water molecule left the first hydration shell of the magnesium ion. This observation is in absolute agreement with experimental findings, that attribute an average residence time of $\approx 2 \times 10^6-10^7$ ps to the water molecules in the first hydration shell of this ion.[40]

From the results presented in Table 2 we may conclude that the MRT decreases with the increase of the electrolyte concentration. This phenomenon can be explained by the stronger competition between the ions to coordinate the fewer accessible water molecules in the more concentrated solution. In the more dilute solution, the larger number of water molecules accessible for each ion allows for keeping the hydration sphere longer and more protected from the influence of nearby ions.

The influence of the interface in the MRT of the water molecules in the hydration shell of the ions is nontrivial and depends on the considered ion. The magnesium ions near the interface can coordinate the ketone oxygens, which are pointing to the aqueous phase. We calculated the average number of ketone oxygens in the first coordination shell of Mg^{2+} near the interface, and a number of ≈ 0 and 0.56 was obtained for, respectively, the 1 and 3 M solutions (numbers obtained by integration of the corresponding radial distribution functions). The latter has a larger coordination number due to the greater number of ions at the interfacial region in competition to coordinate the few water molecules accessible for each ion. Obviously, the coordination of ketone oxygens induces a decrease in the MRT of the water molecules in the ionic hydration shell. In contrast, the increase in the H_2O/ion ratio near the interface contributes to the increase in the MRT of the water molecules in that region. Those effects can explain the increase in the MRT near the interface in the more dilute solution (where there is no coordination of ketone oxygens by the magnesium ions) and the decrease of the MRT near the interface in the more concentrated solution, where the effect of the coordination by the ketone oxygens seems to prevail.

In the case of the chloride ions we cannot expect a coordination by the negative ketone oxygens. Therefore, it should be expected that the MRT would increase near the interface as a consequence of the increase of the H_2O/ion ratio. This is what happens in the more concentrated solution. In the less concentrated solution the MRT decreases near the interface. This seems a little bit surprising, although numerical uncertainty can eventually be responsible for that inversion, considering the closeness of the results and the standard deviations obtained. Further investigation with even better statistics is required to better explain this last observation.

IV. Conclusions

In this paper we have analyzed the properties of an interface between two immiscible electrolyte solutions, namely the interface between 2-heptanone and water, with magnesium chloride as the supporting electrolyte. Two different concentrations of $MgCl_2$ were considered, namely 1 and 3 mol·dm^{-3}.

The density profiles of the solvents show that the existence of the supporting electrolyte slightly shortens the thickness of the interface. Magnesium chloride is a "structure making" salt, and increases the aggregation of the water molecules, thus making the aqueous phase less miscible with the organic solvent.

The ionic density profile decays from the bulk value until almost zero at the interface. The decay starts at ≈ 10 Å from the interface in the 1 mol·dm^{-3} solution and at ≈ 15 Å from the interface in the 3 mol·dm^{-3} solution. The cationic and anionic number density profiles are statistically equivalent; i.e., the number density of the chloride ion always corresponds to twice the number density of the magnesium ion (within statistical accuracy).

Two other related works[51,52] also describe the ionic density profile along the normal to a liquid|liquid interface. However, the description of the interfacial region considered in those works (obtained by calculations based on the density functional formalism for fluids) included a mixed-solvent region with a thickness of several molecular diameters and not a sharp interface, as the one obtained here (and also obtained in all molecular dynamics or Monte Carlo simulations of real fluids). A consequence of that broad interface is that the ions are found to penetrate in the mixed-solvent region, which results in an overlap of the ionic density profiles of the ions belonging to different phases. The overlap region was found to increase with increasing ionic concentration. Those results are coherent with ours, since in our case the mixed-solvent region has a thickness of only 1.0 Å,[14] and consequently the ionic density profiles still penetrate, but only very slightly, the organic phase adjacent to the interface. It was also verified in this work that penetration increases with increasing ionic concentration.

The electric field and the potential drop across the interface were calculated from the charge density profile normal to the interfacial plane. It was found that the electric field was null across almost all the extension of the simulation box. The exception corresponds to a region of about 10 Å thickness at the interfacial zone, where a well demarcated electric field was detected. The existence of this electric field is due to the anisotropic orientation of the solvents, with the water molecules pointing their dipole moments to the organic phase, making hydrogen bonds with the ketone oxygens, which in turn are mainly pointing to the aqueous phase. The ions do not contribute to this electric field, since the net result of the ionic charge is null across all the extension of the simulation box, a consequence of the equivalence between the spatial distribution of cations and anions. The potential drop profile is almost monotonic, decreasing from the organic phase to the water phase, and displaying a small minimum at ≈ 2 molecular diameters inside the water phase. The net potential drop across the interface (HPT2 $\rightarrow$ H_2O) was estimated as -1.1, -1.0, and -1.0 V for the pure system, for the 1 M solution, and for the 3 M solution, respectively.

The density of the solutions of magnesium chloride in the bulk region shows good agreement with experimental data, with a deviation from the experimental result of 2.4% and 4.4% for the less and more concentrated solutions, respectively. This result is a expressive indicator of the quality of the methods and molecular models employed.

The influence of the supporting electrolyte under the specific orientation of the solvents near the interface was evaluated, and it was concluded that the ions are usually too distant from the interface to have a visible influence on the anisotropic orientations of the solvents in that region.

The structure of the hydration shell of the ions as well as the cationic$-$anionic associations were studied at several locations relative to the interfacial plane by calculating the corresponding radial distribution functions. It was noticed that the hydration numbers decreased in the more concentrated solution, where a proportion of only 6.1 water molecules for each ion exists, whereas in the more dilute solution that proportion corresponds to 18.2 water molecules for each ion. This reduced water/ion ratio is the main cause for the decrease in the average hydration number. Surprisingly, this quite logical and intuitive effect seems not to be detected by X-ray reflectivity measurements, where the hydration numbers of Mg^{2+} keep their infinite dilution values in solutions with concentrations up to 4.8 mol·dm^{-3} (a water/ion ratio of 3.8 and a hydration number of 6).

The $Mg^{2+}-Cl^-$ coordination number was found to decrease from bulk solution to the interfacial region (from 0.67 to 0.45 in the 1 M solution and from 1.8 to 0.9 in the 3 M solution).

The decrease is a consequence of the much smaller ionic density near the interface. However, the decrease was found to be quite small when compared to the decrease in the ionic density (13.5 times and 17.2 times, respectively), showing that the cationic−anionic associations are quite stable and robust.

The dynamic properties of the supporting electrolyte were also studied. The diffusion coefficients of both ions were calculated in the bulk region and near the interface. The calculations were performed separately for displacements toward the interface and parallel to the interfacial plane. It was observed that diffusion toward the interface is slower than parallel to the interfacial plane. This anisotropy is the most long-range effect induced by the interface, as it propagates to all extension of the simulation box, and is caused by the impenetrability of the organic phase, which enhances molecular displacements in its direction. Diffusion is faster near the interface than in the bulk region, a consequence of the lower density of the system in that region. This last factor also explains the observed slower dynamics of the ions in the system with the larger ionic concentration, which has also the greater density.

The mean residence time of the water molecules in the first hydration shell of Cl^- and in the second hydration shell of Mg^{2+} was also estimated, both in bulk solution and near the interface. The water molecules belonging to the first hydration shell of Mg^{2+} never left the hydration sphere during all the simulations, in agreement with experimental estimates of the mean residence time of the first hydration shell of Mg^{2+}, which are far superior (by 3 orders of magnitude) to the simulation time. The mean residence times were calculated to be smaller in the more concentrated solution, a fact that can be attributed to the decrease in the H_2O/ion ratio, which enhances the competition for the capture of the few water molecules by the ions.

Acknowledgment. Helpful discussions with Prof. A. Fernando Silva of this department are gratefully acknowledged.

References and Notes

(1) Honig, B. H.; Hubbell, W. L.; Flewelling, R. F. *Annu. Rev. Biophys. Chem.* **1986**, *15*, 163.
(2) Arai, K.; Ohsawa, M.; Kusu, F.; Takamura, K. *Bioelectrochem. Bioenerg.* **1993**, *31*, 65.
(3) Koryta, J.; Skalicky, M. *J. Electroanal. Chem.* **1987**, *229*, 265.
(4) Cunnane, V. J.; Schiffrin, D. J.; Beltran, C.; Geblewicz, G.; Solomon, T. *J. Electroanal. Chem.* **1988**, *247*, 203.
(5) Bell, A.; Frey, J.; VaVandernoot, T. *J. Chem. Soc., Faraday Trans.* **1992**, *88*, 2027.
(6) Grubb, G.; Kim, M.; Raising, T.; Shen, Y. *Langmuir* **1988**, *4*, 452.
(7) Stanners, C.; Du, Q.; Chin, R.; Cremer, P.; Somorjai, G.; Shen, Y. *Chem. Phys. Lett.* **1995**, *232*, 407.
(8) Goth, M.; Hicks, J.; Kemnitz, K.; Pinto, G.; Heinz, T.; Bhattacharyya, K.; Einsenthal, K. *J. Chem. Phys.* **1988**, *92*, 5074.
(9) Eisenthal, K. B. *Chem. Rev.* **1996**, *96*, 1343.
(10) Mitrinovic, D.; Zhang, Z.; Williams, S.; Huang, Z.; Schlossman, M. *J. Phys. Chem. B* **1999**, *103*, 1779.
(11) Michael, D.; Benjamin, I. *J. Electroanal. Chem.* **1998**, *450*, 335.
(12) Benjamin, I. *J. Chem. Phys.* **1992**, *97*, 1432.
(13) Chang, T.; Dang, L. X. *J. Chem. Phys.* **1996**, *104*, 6772.
(14) Fernandes, P. A.; Cordeiro, M. N. D. S.; Gomes, J. A. N. F. *J. Phys. Chem. B* **1999**, *103*, 6290.
(15) Berendsen, H. J. C.; Postma, J. P. M.; van Gunsteren, W. F.; Hermans, J. In *Intermolecular Forces*; Pullman, B., Ed.; Reidel: Dordrecht, 1981; p 331.
(16) Ryckaert, J.; Ciccotti, G.; Berendsen, H. *J. Comput. Phys.* **1977**, *23*, 327.
(17) Fernandes, P. A.; Cordeiro, M. N. D. S.; Gomes, J. A. N. F. *J. Phys. Chem. B* **1999**, *103*, 1176.
(18) Brooks, B. B.; Bruccolery, R. E.; Olafson, B. D.; States, D. J.; Swaminathan, S.; Karplus, M. J. *J. Comput. Chem.* **1983**, *4*, 187.
(19) Pearlman, D. A.; Case, D. A.; Cadwell, J. C.; Seibel, G. L.; Sing, U. C.; Weiner, P.; Kollman, P. A. *AMBER4*; University of California: San Francisco, 1991.
(20) Åqvist, J. *J. Phys. Chem.* **1990**, *94*, 8021.
(21) Straatsma, T. P.; Berendsen, H. J. C. *J. Chem. Phys.* **1988**, *89*, 5876.
(22) van Gusteren, W. F. *GROMOS Reference Manual*; BIOMOS B. V.: Nijenborgh 16, Groningen, The Netherlands, 1987.
(23) Hoover, W. G. *Phys. Rev. A* **1985**, *A31*, 1695.
(24) Melchionna, S.; Ciccotti, G.; Holian, B. L. *Mol. Phys.* **1993**, *78*, 533.
(25) Forrester, T. W.; Smith, W. *Mol. Simul.* **1994**, *13*, 195.
(26) Forrester, T. W.; Smith, W. *DLPOLY*, 2.6 version; CCLRC: Daresbury Laboratory, 1995.
(27) Fernandes, P. A.; Cordeiro, M. N. D. S.; Gomes, J. A. N. F. *J. Phys. Chem. B* **1999**, *103*, 8930.
(28) *Handbook of Chemistry and Physics*; Weast, R. C., Ed.; CRC Press: Boca Raton, FL, 1989.
(29) Pratt, L. R. *J. Chem. Phys.* **1992**, *96*, 25.
(30) Wilson, M. A.; Pohorille, A.; Pratt, L. R. *J. Chem. Phys.* **1988**, *88*, 3281.
(31) Frenkel, J. *Kinetic Theory of Liquids*; Oxford: Clarenton, 1955.
(32) Stillinger, F. H.; Ben-Naim, A. *J. Chem. Phys.* **1967**, *47*, 4431.
(33) Bol, W.; Gerrits, G. J. A.; van Panthaleon van Eck, C. L. *J. Appl. Crystallogr.* **1970**, *3*, 486.
(34) Dorosh, A. K.; Skryshevskii, A. F. *J. Struct. Chem.* **1964**, *5*, 842.
(35) Caminiti, R.; Licheri, G.; Piccaluga, G.; Pinna, G. *J. Appl. Crystallogr.* **1979**, *12*, 34.
(36) Caminiti, R.; Licheri, G.; Piccaluga, G.; Pinna, G. *Z. Naturforsch.* **1980**, 1361.
(37) Pálinkás, G.; Radnai, T.; Dietz, W.; Scász, G. I.; Heizinger, K. *Z. Naturforsch.* **1982**, 1049.
(38) Licheri, L.; Piccaluga, G.; Pinna, G. *J. Appl. Crystallogr.* **1973**, *6*, 392.
(39) Powell, D. H.; Neilson, G. W.; Enderby, J. E. *J. Phys. Condens. Matter* **1993**, *5*, 5723.
(40) Ohtaki, H.; Radnai, T. *Chem. Rev.* **1993**, *93*, 1157.
(41) Caminiti, R. *J. Mol. Liq.* **1984**, *28*, 191.
(42) Caminiti, R.; Cucca, P.; Monduzzi, M.; Sabba, G.; Crisponi, G. *Chem. Phys.* **1984**, *81*, 543.
(43) Yamaguchi, T.; Hayashi, S.; Ohtaki, H. *Inorg. Chem.* **1989**, *28*, 2434.
(44) Hertz, H. G. In *Water—A Comprehensive Treatise*; Franks, F., Ed.; Plenum: New York, 1973; Vol. 3, Chapter 4, p 191.
(45) Hewish, N. A.; Howells, W. S. *J. Phys. C.: Solid State Phys.* **1983**, *16*, 1777.
(46) Sprik, M.; Klein, M.; Watanabe, K. *J. Phys. Chem.* **1990**, *94*, 6483.
(47) Berendsen, H. J. C.; Grigera, J. R.; Straatsma, T. P. *J. Phys. Chem.* **1987**, *91*, 6269.
(48) Jorgensen, W.; Chandrasekhar, J.; Madura, J. D.; Impey, R.; Klein, M. *J. Chem. Phys.* **1983**, *79*, 926.
(49) Impey, R. W.; Madden, P. A.; McDonald, I. R. *J. Phys. Chem.* **1983**, *87*, 5071.
(50) Garcia, A. E.; Stiller, L. *J. Comput. Chem.* **1993**, *14*, 1396.
(51) Pereira, C. M.; Schmickler, W.; Silva, A. F.; Sousa, M. J. *J. Electroanal. Chem.* **1997**, *268*, 13.
(52) Huber, T.; Pecina, O.; Schmickler, W. *J. Electroanal. Chem.* **1999**, *467*, 203.